Multi-scale/multi-fluid simulations of the post plasmoid current sheet in the terrestrial magnetosphere

E. M. Harnett,[1] R. M. Winglee,[1] and C. Paty[1]

Received 27 June 2006; revised 24 August 2006; accepted 4 October 2006; published 11 November 2006.

[1] Multi-scale/multi-fluid simulations are used to provide the first high resolution (~120 km) simulations of a thin tail current sheet within the global framework of the Earth's magnetosphere during southward IMF. The current sheet in the tail is shown to thin to 1200 km in the wake of a plasmoid. A hydrogen boundary layer forms on the outside of the current sheet with a thickness on the order of 900 km. Kinks form in the cross-tail direction in the thin current sheet with a wavelength on the order of 1 R_E. The amplitude grows up to 0.5 R_E before the kinks become unstable, leading to the reformation of a thicker current sheet. These kinks initiate just earthward of the reconnection region and propagate both tailward, and earthward until they reach dipolar fieldlines. These processes occur as the result of the coupling between cross-tail flows in O^+ and field-aligned flows in ionospheric H^+. **Citation:** Harnett, E. M., R. M. Winglee, and C. Paty (2006), Multi-scale/multi-fluid simulations of the post plasmoid current sheet in the terrestrial magnetosphere, *Geophys. Res. Lett.*, *33*, L21110, doi:10.1029/2006GL027376.

1. Introduction

[2] The theory of magnetic reconnection as a means for producing energetic particles has nearly 6 decades of history. *Giovanelli* [1948] first proposed that reconnection might be driving accelerated particles in solar flares. Application of the reconnection regions to the terrestrial space environment lead to the *Dungey* [1961] model which was able to predict many of the large-scale features of the magnetosphere. Magnetic reconnection plays a critical role in determining the morphology of the magnetotail particularly during substorms and storms. The early models quickly recognized that the reconnection rate from Coulomb collisions was orders of magnitude too slow, and hence anomalous resistivity due to wave-particle interactions was introduced to produce enhanced scattering of particles consistent with observed reconnection rates. However, *Drake et al.* [1994] showed for idealized geometries that reconnection does not occur in a smooth MHD manner but rather occurs through filamentation and kinking of the current sheet. And comparison of 2D particle, hybrid, Hall MHD, and ideal MHD simulations of reconnection in a Harris current sheet [*Birn et al.*, 2001, and references therein] showed that all models that included the Hall term in Ohm's law predicted similar reconnection rates, regardless of the mechanism that initiated reconnection.

[3] Associated with reconnection is the development of thin current sheets. Thin current sheets have been observed during substorms [cf. *Sergeev et al.*, 1990, 1993; *Mitchell et al.*, 1990; *Lui et al.*, 1992; *Asano et al.*, 2003], with a thickness on the order of ~1000 km, or comparable to the ion inertial length. In the past, such thin current sheets have only modeled for small regions of the magnetosphere. 2D simulations of the tail region employing particle-in-a-cell models [cf. *Pritchett and Coroniti*, 1994; *Hoshino et al.*, 1998], hybrid models [cf. *Hesse et al.*, 1996; *Arzner and Scholer*, 2001] and Hall MHD models [cf. *Ma and Bhattacharjee*, 1998; *Rastätter et al.*, 1999] all showed the development of thin current sheets after reconnection. But these models were limited in that they could only show structure along the tail. 3D particle and hybrid simulations of the tail [*Zhu and Winglee*, 1996; *Pritchett and Coroniti*, 2001; *Karimabadi et al.*, 2003] showed the development of cross-tail structure such as kinks and filamentation.

[4] In this paper we present results from multi-scale/multi-fluid simulations that fully resolve thinning of the current sheet and disruption by kinking of the tail current sheet during southward IMF conditions. These results represent a major advance in magnetospheric modeling because they can show features with scale sizes on the order of a few hundred kilometers within the context of a global system. The predicted scale sizes of current sheet and boundary layer thickness agree with satellite observations. Predicted kinking wavelengths and amplitudes have implications for optimal spacecraft orientations during the upcoming MMS mission to study reconnection in the magnetotail.

2. Model

[5] Reconnection within a global multi-fluid model that includes heavy ion and ion cyclotron dynamics has shown the presence of substantial dawn-dusk asymmetries owing to mass loading of the dusk side from heavy ions following Speiser-like orbits across the tail current sheets [*Winglee*, 2004]. These simulations were the first to obtain consistent macroscopic flows derived from global simulations with those obtained from single particle tracking [*Winglee*, 2003]. The multi-fluid simulations were able to demonstrate the generation of small scale (~2 R_E) flux ropes that do not appear in any global MHD model, which have properties similar to those inferred from previous tail observations [*Winglee*, 2004]. Subsequent modeling has been able to demonstrate that the timing and spatial distribution of the heavy ion outflows from the multi-fluid model are consistent with IMAGE/HENA data [*Winglee et al.*, 2005].

[6] The simulations presented in this paper use the multi-fluid technique [*Winglee*, 2004] but also utilize a refined

[1]Department of Earth and Space Sciences, University of Washington, Seattle, Washington, USA.

0094-8276/06/2006GL027376$05.00

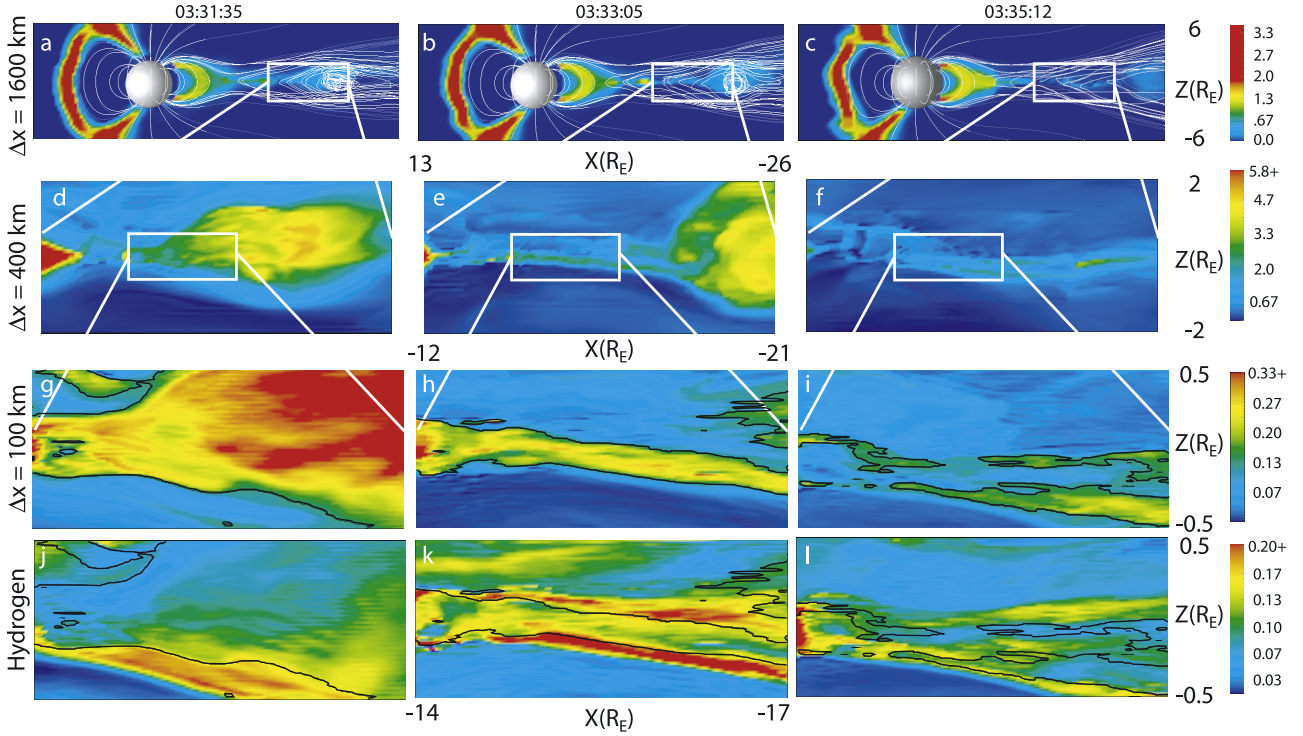

Figure 1. The evolution of the electron pressure in the noon-midnight meridian showing a meso-scale flux rope and the development of a thin current sheet in its wake. All pressures are in units of nPa. The bottom row is the hydrogen pressure at the same location as the electron pressure in row three. The contour line shown in row three is replicated in row four and is equal to 0.13 nPa. The silver sphere is row one indicates the inner boundary at a 2.5 R_E.

gridding technique to yield local grid resolutions of 100 km (and comparable to the ion inertial length) in the magnetotail of a global multi-fluid simulation. This is accomplished by first establishing a global equilibrium at coarse (1/4 R_E) resolution for non-substorm/non-storm conditions. The system is then driven by the desired solar wind conditions. At key times the refined gridding system is initiated around the region of interest to desired resolution. Plasma and field quantities are passed between grid systems at each time step ensuring full coupling between the grid systems. This makes the code not only multi-fluid but also multi-scale and allows us to investigate the roles of plasma beta and external forcing on the evolution of the current sheet/reconnection region within the global context.

[7] The simulations incorporate a four-fluid system: one electron fluid, and the solar wind H^+, ionospheric H^+, and ionospheric O^+ ion components. The solar wind conditions represent nominal southward IMF conditions. The solar wind density is set to 6 cm^{-3} with a speed of 650 km/s. The system was driven with constant southward IMF with a magnitude of 5 nT. The inner boundary is set at 2.5 R_E. The electron pressure is initialized at half the ion pressure but then is allowed to vary in time. A detailed description of the equations solved can be found in the work by *Winglee* [2004].

3. Results

[8] Figure 1 shows the fast evolution of the development of a flux rope and a thin current sheet in its wake. For clarity, the top panels only show the inner part of the magnetosphere (coarsest resolution in the region is 1600 km). In the lower panels we show additional close ups at increasingly higher spatial resolution. The grid resolution jumps by only a factor of two between successive grid systems but to keep the image simple only every other grid system is shown. At time 03:31:35, a meso-scale (3 R_E full width) flux rope can be seen at the right hand side of the image. This flux rope is traveling at a speed of about 500 km/s and is seen to expand as it moves down the tail. This scale size and speed is consistent with observations of flux ropes with sizes of 1–4 R_E by Geotail and Cluster [*Slavin et al.*, 2003a, 2003b]. In its wake, a thin, 1200 km wide, current sheet forms. Using Cluster data, *Nakamura et al.* [2002] demonstrated thinning of the current sheet from about 1 R_E thick to about 400 km, which they note is close to the ion inertial length. For such thin current sheets, the Hall term in the generalized Ohm's law becomes non-negligible. These corresponding Hall currents have recently been confirmed by Geotail observations [*Nagai et al.*, 2003].

[9] As we zoom into the flux rope structure at higher resolution, micro-scale structures are seen that are barely resolved at 400 km resolution but are fully resolved at 100 km resolution. At 600 km half width, the thin current sheet is numerically resolved in the finest grid system, though higher resolution may provide a few sharper features. Looking at the 100 km images, the thinning rate of the current sheet is ~50 km/s in the z direction, which is also consistent with the above observations.

[10] The cross-tail view behind the flux rope (Figure 2) shows the ability of the tail to support a thin current sheet

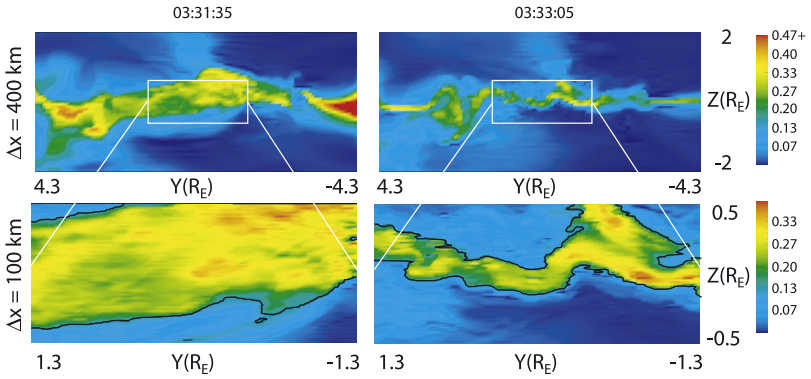

Figure 2. A cross-tail cut of electron pressure looking Earthward at X = −15.7 R_E showing rapid thinning and development of cross-tail kinking. All pressures are in units of nPa. The contour line in the bottom panels is for a value equal to 0.13 nPa.

across a substantial fraction of the tail. Further evidence that the system is resolved is the separation between the electron properties and those of the H^+ and O^+ properties (Figure 3). The electron pressure is predominantly in the center of the current sheet (Figures 1h and 3a). The most energetic protons line on either side on the flanks of the current sheet, producing the plasma sheet boundary layer both along the tail (Figures 1j–1l) and cross the tail (Figure 3b). This hydrogen boundary layer is ∼850 km thick. This separation is consistent with the full particle simulations of *Zhu and Winglee* [1996]. The heavy ions with their much large gyro-radius have broader features which tend to maximize in the center of the current sheet but in the vicinity of the kinks can be the dominant ion contribution to the overall plasma pressure.

[11] As the current sheet thins in the wake of the plasmoid, it is subject to the development of small-scale kinking of the thin plasma sheet (Figures 2 and 3). This type of kinking also consistent with *Zhu and Winglee* [1996] and has been seen by Cluster [*Volwerk et al.*, 2003]. The modeling shows that the wavelength of the kinking ranges from 0.5 to 2 R_E depending on position across the tail. The cyclotron radius of O^+ in this region is between 0.5 R_E and 1.5 R_E, setting the inherent scale-size for the kinks. The amplitude can grow up to 0.5 R_E. As the amplitude of the kinked region approaches 0.5 R_E, the region becomes unstable and the kinks begin to break up, leading to the formation of a thicker current sheet. Both the amplitude and the wavelength are consistent with those measured by Cluster [*Runov et al.*, 2003]. The kinked regions move both tailward, in the wake of the plasmoid and earthward until they reach the more dipolar fieldlines at about 10 R_E. The dipolar fieldlines prevent further earthward propagation of the thin current sheet.

[12] This kinking occurs after strong cross-tail flows of O^+ but is driven by the difference in direction of the flow of the light and heavy ions. Prior to the development of the kinks, the flow of ionospheric H^+ is primarily field-aligned and perpendicular to that of O^+. When the O^+ concentration is increased in the tail, kinking in the tail does not form as readily, but once it forms the wavelength and amplitude of the kinked region is bigger. The delay in onset of kinking is because the higher concentration of the heavier mass O^+ means it takes longer for the plasma as a whole to reach the energy necessary for kinking to develop. The affect of O^+ on the dynamics is important because the composition of the tail is not static. In their study of the inner magnetosphere using CRRES, *Korth et al.* [2002] showed that storm-time substorms can have ratios of O^+/H^+ of several hundred percent while non-storm-time substorms have ratios of O^+/H^+ 15–65%. Even for these values, O^+ is a significant factor to the total energy density. Recent observations from the Cluster mission have shown that during geomagnetically disturbed times, thin current sheets are observed. Within them the O^+ number density close to the reconnection X-line in the Earth's magnetotail can become comparable to, or even higher than, the corresponding H^+ number density, and that the O^+ ions carry most of the particle pressure [*Kistler et al.*, 2005].

[13] One of the major features of the multi-fluid code is that it is able to provide energy spectrograms at the same

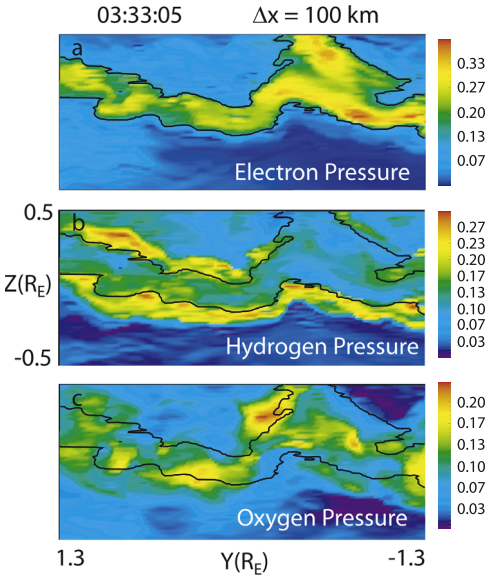

Figure 3. Cross-tail cuts at high resolution of the pressure of (a) electrons, (b) H^+ and (c) O^+. The black contour line is at an electron pressure equal to 0.13 nPa and is replicated in the bottom other panels for relative comparison with H^+ and O^+. All pressures are in units of nPa.

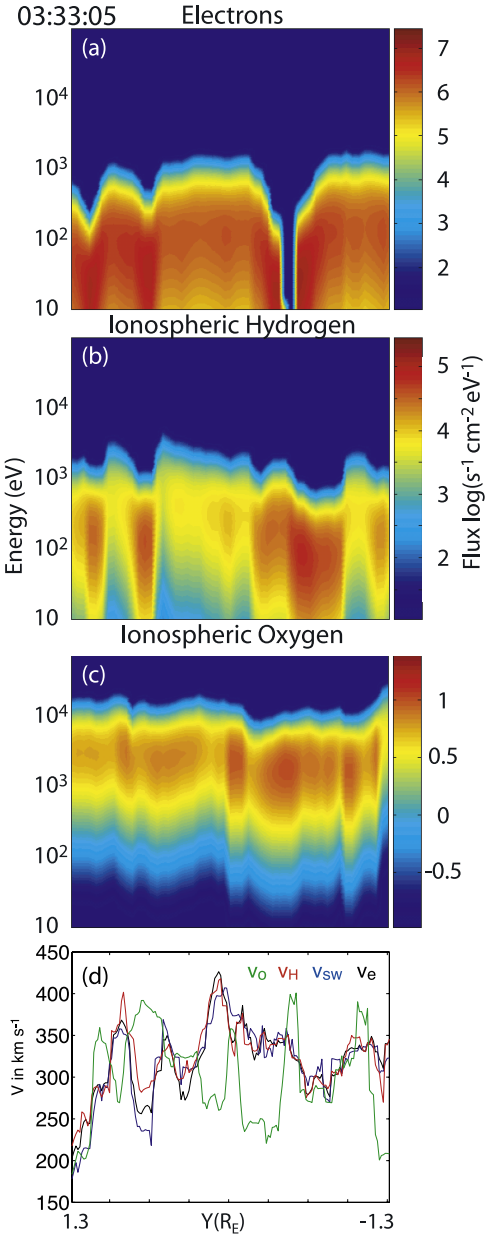

Figure 4. Energy spectrograms for e, H^+ and O^+ through a cut across the middle of the plane shown in Figure 3. Also shown are the bulk velocities of O^+ (green), ionospheric H^+ (red), solar wind H^+ (blue) and the electron drift velocity (black) at the same locations that the spectrograms are taken at.

resolution of the grid spacing. This spectrogram is derived from the inferred number density (n^i), velocity (v_b^i) and temperature (v_T^i) of each species i. Assuming a Maxwellian distribution, the flux for each species can be calculated at a given point, $\vec{x}$, between a range of energies, E, which corresponds to a velocity, v_o^i, for a given mass, m^i:

$$f^i\left(\vec{x}, v_o^i\left(E, m^i\right)\right) = \frac{\left(v_o^i\right)^2}{m^i} \frac{\eta m^i}{\left(v_T^i\right)^3} \exp - \frac{\left(v_o^i - v_b^i\right)^2}{2\left(v_T^i\right)^2} \qquad (1)$$

where η is the normalization. Figure 4 shows spectrograms for three different species along a synthetic trajectory taken at Z = 0 in the same planes shown in Figure 3. Note that if one were to plot spectrograms over consecutive grid points (not shown due to space limitations) one could easily verify variations at the 200+ km range. The spectrograms clearly show that oxygen is preferentially energized by nearly an order of magnitude in energy as compared to hydrogen (Figure 4c vs Figure 4b). This means that as there is a different spatial distribution of the heavy ions relative to the light ions. This is further highlighted in the velocity profiles (Figure 4d). The O^+ bulk speed is anti-correlated with the light ion and electron bulk speed. Also note the fast flow speeds - the largest contribution of which comes from the tailward flow. The immersion of flux ropes in fast flows is noted by *Slavin et al.* [2003a], with the speeds comparable to those seen by *Tu et al.* [1997] in the post plasmoid current sheet.

[14] At locations that the trajectory enters the current sheet, the peak energy increases and the flux decreases. This is most evident in the electrons and hydrogen (Figures 4a and 4b). The larger cyclotron radius of the oxygen makes the features in the spectrogram (Figure 4c) less distinct. The drop-out in the electron flux (Figure 4a) is a result of the trajectory sampling the edge of the low temperature region that forms below the current sheet. Cross tail kinks lead to the decreases in the peak energy of the light ions to a much greater extent than the heavy ions, with the flux of ionospheric hydrogen varying by two orders of magnitude while the oxygen flux varies only by a factor or 10.

4. Conclusions

[15] These results demonstrate that a multi-scale/multi-fluid treatment can yield very similar results to particle treatments, while being able to establish them within the global environment and without the time and spatial ambiguities inherent with local models. This is important for determining how the processes initiated in a small region by reconnection in the tail can propagate out into the global magnetosphere. The results also demonstrate that the structure of thin current sheets has been very much oversimplified in the past. Incorporating grid resolutions on the order of 100 km not only affect the results by being able to resolve structures with scale sizes on the order of 1000 km, it affects the global results as these small scale structures grow and propagate throughout the tail region. This leads to much better agreement between model results and satellite observations and goes a long way in advancing the study of dynamics in the terrestrial magnetosphere.

[16] **Acknowledgment.** This work was funded by a NSF GEM Fellowship and a NASA Geospace grant.

References

Arzner, K., and M. Scholer (2001), Kinetic structure of the post plasmoid plasma sheet during magnetotail reconnection, *J. Geophys. Res.*, *106*, 3827–3844.

Asano, Y., T. Mukai, M. Hoshino, Y. Saito, H. Hayakawa, and T. Nagai (2003), Evolution of the thin current sheet in a substorm observed by Geotail, *J. Geophys. Res.*, *108*(A5), 1189, doi:10.1029/2002JA009785.

Birn, J., et al. (2001), Geospace environmental modeling (GEM) magnetic reconnection challenge, *J. Geophys. Res.*, *106*, 3715–3720.

Drake, J. F., et al. (1994), Structure of thin current layers: Implications for magnetic reconnection, *Phys. Rev. Lett.*, *73*, 1251–1254.

Dungey, J. W. (1961), Interplanetary magnetic field and the auroral zones, *Phys. Rev. Lett.*, *6*, 47–48.

Giovanelli, R. G. (1948), Chromospheric flares, *Mon. Not. R. Astron. Soc.*, *108*, 163–176.

Hesse, M., et al. (1996), Hybrid modeling of the formation of thin current sheets in the magnetotail, *J. Geomagn. Geoelectr.*, *48*, 749–763.

Hoshino, M., T. Mukai, T. Yamamoto, and S. Kokubun (1998), Ion dynamics in magnetic reconnection: Comparison between numerical simulation and Geotail observations, *J. Geophys. Res.*, *103*, 4509–4530.

Karimabadi, H., P. L. Pritchett, W. Daughton, and D. Krauss-Varban (2003), Ion-ion kink instability in the magnetotail: 2. Three-dimensional full particle and hybrid simulations and comparison with observations, *J. Geophys. Res.*, *108*(A11), 1401, doi:10.1029/2003JA010109.

Kistler, L. M., et al. (2005), Contribution of nonadiabatic ions to the cross-tail current in an O^+ dominated thin current sheet, *J. Geophys. Res.*, *110*, A06213, doi:10.1029/2004JA010653.

Korth, A., et al. (2002), Ion composition of substorms during storm-time and non-storm-time periods, *J. Atmos. Sol. Terr. Phys.*, *64*, 561–566.

Lui, A. T. Y., B. J. Anderson, K. Takahashi, L. J. Zanetti, R. W. McEntire, T. A. Potemra, R. E. Lopez, D. M. Klumpar, E. M. Greene, and R. Strangeway (1992), Current disruptions in the near-Earth neutral sheet region, *J. Geophys. Res.*, *97*, 1461–1480.

Ma, Z. W., and A. Bhattacharjee (1998), Sudden enhancement and partial disruption of thin current sheets in the magnetotail due to Hall MHD effects, *Geophys. Res. Lett.*, *25*, 3277–3280.

Mitchell, D. G., D. J. Williams, C. Y. Huang, L. A. Frank, and C. T. Russell (1990), Current carriers in the near-Earth cross-tail current sheet during substorm growth phase, *Geophys. Res. Lett.*, *17*, 583–586.

Nagai, T., I. Shinohara, M. Fujimoto, S. Machida, R. Nakamura, Y. Saito, and T. Mukai (2003), Structure of the Hall current system in the vicinity of the magnetic reconnection site, *J. Geophys. Res.*, *108*(A10), 1357, doi:10.1029/2003JA009900.

Nakamura, R., et al. (2002), Fast flow during current sheet thinning, *Geophys. Res. Lett.*, *29*(23), 2140, doi:10.1029/2002GL016200.

Pritchett, P. L., and F. V. Coroniti (1994), Convection and the formation of thin current sheets in the near-Earth plasma sheet, *Geophys. Res. Lett.*, *21*, 1587–1590.

Pritchett, P. L., and F. V. Coroniti (2001), Kinetic simulations of 3-D reconnection and magnetotail disruptions, *Earth Planets Space*, *53*, 635–643.

Rastätter, L., M. Hesse, and K. Schindler (1999), Hall-MHD modeling of near-Earth magnetotail current sheet thinning and evolution, *J. Geophys. Res.*, *104*, 12,301–12,312.

Runov, A., R. Nakamura, W. Baumjohann, T. L. Zhang, M. Volwerk, H.-U. Eichelberger, and A. Balogh (2003), Cluster observation of a bifurcated current sheet, *Geophys. Res. Lett.*, *30*(2), 1036, doi:10.1029/2002GL016136.

Sergeev, V. A., P. Tanskanen, K. Mursula, A. Korth, and R. C. Elphic (1990), Current sheet thickness in the near-Earth plasma sheet during substorm growth phase, *J. Geophys. Res.*, *95*, 3819–3828.

Sergeev, V. A., D. G. Mitchell, C. T. Russell, and D. J. Williams (1993), Structure of the tail plasma/current sheet at $\sim$11 R_E and its changes in the course of a substorm, *J. Geophys. Res.*, *98*, 17,345–17,366.

Slavin, J. A., R. P. Lepping, J. Gjerloev, D. H. Fairfield, M. Hesse, C. J. Owen, M. B. Moldwin, T. Nagai, A. Ieda, and T. Mukai (2003a), Geotail observations of magnetic flux ropes in the plasma sheet, *J. Geophys. Res.*, *108*(A1), 1015, doi:10.1029/2002JA009557.

Slavin, J. A., et al. (2003b), Cluster four spacecraft measurements of small traveling compression regions in the near-tail, *Geophys. Res. Lett.*, *30*(23), 2208, doi:10.1029/2003GL018438.

Tu, J.-N., T. Mukai, M. Hoshino, Y. Saito, Y. Matsuno, T. Yamamoto, and S. Kokubun (1997), Geotail observations of ion velocity distributions with multi-beam structures in the post-plasmoid current sheet, *Geophys. Res. Lett.*, *24*, 2247–2250.

Volwerk, M., K.-H. Glassmeier, A. Runov, W. Baumjohann, R. Nakamura, T. L. Zhang, B. Klecker, A. Balogh, and H. Rme (2003), Kink mode oscillation of the current sheet, *Geophys. Res. Lett.*, *30*(6), 1320, doi:10.1029/2002GL016467.

Winglee, R. M. (2003), Circulation of ionospheric and solar wind particle populations during extended southward interplanetary magnetic field, *J. Geophys. Res.*, *108*(A10), 1385, doi:10.1029/2002JA009819.

Winglee, R. M. (2004), Ion cyclotron and heavy ion effects on reconnection in a global magnetotail, *J. Geophys. Res.*, *109*, A09206, doi:10.1029/2004JA010385.

Winglee, R. M., W. Lewis, and G. Lu (2005), Mapping of the heavy ion outflows as seen by IMAGE and multifluid global modeling for the 17 April 2002 storm, *J. Geophys. Res.*, *110*, A12S24, doi:10.1029/2004JA010909.

Zhu, Z., and R. M. Winglee (1996), Tearing instability, flux ropes, and the kinetic current sheet kink instability in the Earth's magnetotail: A three-dimensional perspective from particle simulations, *J. Geophys. Res.*, *101*, 4885–4897.

E. M. Harnett, C. Paty, and R. M. Winglee, Department of Earth and Space Sciences, Box 351310, University of Washington, Seattle, WA 98195-1310, USA. (eharnett@ess.washington.edu; cpaty@u.washington.edu; winglee@ess.washington.edu)